Click to view slide presentation (5.54 MB)

Comparing and Contrasting Analytically Quantified Porosity and Pore Size Distributions in the Wolfcamp Formation From SEM Imaging, Nuclear Magnetic Resonance (NMR), and Crushed Rock Core Analysis*

Stephanie E. Perry[1], Joel D. Walls[2], and Tiffany Rider[2]

Search and Discovery Article #42123 (2017)**
Posted August 14, 2017

*Adapted from extended abstract prepared in conjunction with oral presentation given at AAPG 2017 Annual Convention and Exhibition, Houston, Texas, April 2-5, 2017

[1]Petrophysics, Anadarko Petroleum Corporation, The Woodlands, Texas, United States (Stephanie.Perry@Anadarko.com)
[2]INGRAIN Inc., Houston, Texas, United States

Abstract

Total porosity has been measured using crushed rock shale analysis, ion-milled scanning electron microscope (SEM) imagery, and fresh-state, nuclear magnetic resonance (NMR) in a Delaware Basin case study. One objective of this analysis was to compare results from different methodologies and determine if SEM-quantified pore size distributions can be used to interpret or calibrate fresh-state NMR results with parameters explicit to mimicking open-hole wireline physics. Another objective was to understand how organic vs non-organic pores are or are not detected and quantified by standard analytical methods.

The main application of this work is to quantify organic- vs. non-organic hosted porosity from SEM images and to relate it to fresh-state NMR data. SEM total porosity was compared to crushed rock data from the same samples. The difference between SEM and crushed rock total porosity was directly correlated to clay content with the apparent clay bound water being ~20% of the dry clay bulk volume. Then comparing the differences between fresh-state NMR and SEM-based total porosity, we have quantified the clay-bound water 'correction'. There is a relationship observed between fresh-state NMR T2 and SEM-derived pore size distributions. However, fresh-state NMR response is dominated by non-organic rather than organic hosted pores (physical limitations of techniques).

Understanding the relationships between these different analytical techniques and resulting quantification is key to relating various pore-scale systems in horizontally-stimulated source rock reservoirs. Defining the link through correlation between fresh-state NMR data, SEM imaging, and crushed rock analysis for shale evaluation could help resolve the challenging 'up-scaling' limitations the industry commonly encounters.

Key observations and conclusions from this work are: 1) SEM analysis can be used to quantify organic and non-organic porosity, 2) Crushed-rock total porosity for these samples included a substantial clay-bound water component that was directly correlated to x-ray fluorescence

(XRF) clay volume, 3) Dry helium porosity and SEM porosity plus computed clay-bound water porosity compare favorably, 4) Fresh-state NMR total porosity plus SEM organic porosity best matched the clay-bound water corrected SEM porosity, helping bridge the gap between independent techniques exploiting various analytical methodology to arrive at a consistent and reliable porosity quantification.

Introduction

The Wolfcamp Formation in the Delaware Basin continues to be a major economic and geologic target for US E&P operators. While lower commodity prices have resulted in major cuts to drilling programs in many North America shale formations, the Wolfcamp Formation has experienced little in the way of reduced exploitation activity. With hundreds of wells drilled, logged, cored, and completed in the last few years, there continues to be many questions about its basic rock properties, storage, and flow potential. The high vertical variability of the formation results in significant changes in rock properties along a drilled lateral path as the drill bit may cross multiple bed boundaries simply by oscillating up and down within a few (<3-5) vertical feet (TVD/MD').

The heterogeneity makes it critical to have a good understanding of the reservoir properties over a wide range of existing rock types. In particular, it is important to know the storage capacity for hydrocarbons and how this varies with changes in lithology. In this project, core samples and log data were used to quantify total, effective and organic-associated porosity through the application of multiple techniques. The interval studied contained plug samples from 41 depths and were analyzed using digital rock methods as well as traditional crushed-rock type core analysis. Open-hole wireline nuclear magnetic resonance (NMR) log data were acquired and complimented by lab-based NMR porosity on as-received 0.92-1 inch diameter conventional plug samples.

Geologic Setting

The Permian Basin has long been a prolific hydrocarbon producing system, first through targeting and completion of vertical, conventionally defined reservoirs and second, (more recently) via the application of horizontal drilling and completion technology to target unconventional, source-reservoir, interbedded stratigraphy. The basin resulted from subsidence, accumulation, and relaxation after the North and South American Gondwanian collision (~310-265 Ma).

Specifically the Delaware Basin, West Texas, has become the target for emergence of renewed hydrocarbon resource production and continues to thrive as knowledge, understanding, and technology advances in horizontal stimulation of unconventional, hybrid (thinly-bedded) targeted reservoirs. The basin contains multiple unconventional shale deposits including the Woodford, Wolfcamp, and Avalon stratigraphy. The Wolfcamp Shale is a major oil and gas producing formation in Texas. In 2015 oil production from the Permian region exceeded 2 million BOPD and a large fraction of it was produced from the Wolfcamp Formation.

The Delaware Basin has a prolonged tectonic history with a number of major collisional and extensional events of significance from the Cambrian through the Miocene. The Wolfcampanian marks a time of significant basin subsidence and hinterland uplift driving greater than ~8000 feet of sedimentary deposition. The deposition into the basin alternated between clastic-dominated turbiditic provenance from the

northwest, west, and southwest to carbonate slumping, debris flow, and mass wasted carbonate shelf margins along the west, northwest, and eastern margins.

The case study focuses on stratigraphy that is microporosity-dominated with permeability ranging from nano-to millidarcies and is related to the deposition of argillaceous, siliceous dominated turbiditic sequences with diagenetic overprinting and includes carbonaceous-dominated basal debris flows in a variable slope to basin setting through time.

Samples and Methods

The project consisted of 41 as-received 0.92-1 inch diameter conventional plug samples. Archimedes bulk density was measured on as-received samples. Porosity was measured as-received and then on solvent-extracted, dried samples using a crushed-rock type method as described in Luffel et al., 1995. LECO TOC and basic RockEval parameters were obtained on nearby samples. A subset of these 41 samples were also analyzed for as-received NMR porosity (Oxford instruments Maran Ultra) at ambient conditions with a 0.2 ms echo spacing, standard CPMG pulse sequence, and a SNR of 100:1 with Tau of 100 µs. An analog filter was used for ~100,000Hz range.

No micro-cracks or degradation in plug quality was observed on CT-Scans of the plugs prior to the study. Temperature was closely monitored during the experimentation. Pre-test discrepancy between Archimedes bulk density and caliper-based bulk densities was observed and rectified prior to continuing the experimental components of the study (Figure 1).

To aid with sub-sample selection for complimentary SEM imaging, five X-ray fluorescence (XRF) measurements were acquired along the vertical axis of the plug end trim, perpendicular to bedding. The end trims were polished and sets of high resolution X-ray CT projections (20 microns and 4 microns per voxel) were used to observe each samples heterogeneity and locate an area to prepare for the SEM.

All sub-samples were extracted and polished with an argon-ion-beam milling system. Images of the polished areas, approximately 1 millimeter by 0.5 millimeter, were captured using a SEM secondary electron (SE2) detector at a resolution of 250 nanometers per pixel. Next, a series of images at a resolution of 10 nanometers per pixel were acquired simultaneously using both the SE2 and back-scatter electron detectors. These higher resolution SEM images were acquired perpendicular to bedding, along the vertical axis.

The sets of high-resolution images were combined and segmented for porosity (PhiE), organic matter (OM), higher density minerals, and matrix grains. The porosity was further analyzed and separated into porosity associated with organic material (PAOM) and mineral-associated porosity (intergranular plus intragranular). Figure 2A shows a SE2 SEM image from one sample used in the study. Figure 2B shows the segmentation of the same image with colors indicating OM, PAOM, and mineral-associated porosity.

Results and Discussion

Organic vs. non-organic hosted porosity from SEM images was compared to fresh-state NMR and crushed rock data from the same aliquoted sample mass. From a selected subset of samples, high resolution SEM images were acquired at 2.5nm/pixel and segmented for PhiE, OM,

PAOM. The high resolution images were compared to the same area from the 10nm/pixel SEM image to identify additional small pores and to better define the pores associated with organics and clays. The average fractional porosity difference between 2.5 and 10 nm/pixel images was used to compute a resolution corrected image porosity (quantification based on pore mapping and summation) for each sample. The largest difference between SEM porosity and crushed rock porosity (helium porosimetry technique through 20/35 mesh crushed aliquot) was directly correlated to total clay content (Figure 3A).

From Dean-Stark water saturation, the bulk volume water was determined and this value was compared to total clay volume from XRF (Figure 3B). Clay-bound water volume was approximately 20% of the clay bulk volume. The intercept of this data is near zero suggesting that most water in these samples is associated with clay surface area. Variability around the trend is expected and depends on variations in high versus low surface area clays in each sample. By comparing fresh-state Dean-Stark fluid saturations and SEM porosity, we have quantified the clay-bound water correction. The SEM image resolution is not high enough to discriminate the clay-bound water so it is not counted as pore space. Therefore to compare SEM porosity to dry helium porosity (where the clay bound water is driven off by drying), we have added the computed clay bound water volume to the SEM image porosity. This computed PhiT_DRA porosity compares favorably to the dry helium porosity (Figure 3C).

The majority of samples in this study are microporosity dominated. All major pore types, inter-granular, intra-granular, and organic-hosted are present. See Figure 4 and Figure 5 (modified from Loucks et al. 2015). This hybrid reservoir system is dominated by phyllosilicate and intra- to inter-granular pores, with organic pores making up about 37% of the porosity available for hydrocarbon storage.

Fresh-state plug samples from this well were analyzed for NMR porosity as described in the methods section. The PhiT_DRA is overall higher by about 31% than the fresh-state plug sample NMR porosity (Figure 6). Another comparison shows that dry helium porosity is about 35% higher than NMR porosity. The difference may be related to porosity associated with organic material and evaluated fluid-filled pore volume under as-received conditions. It is likely that the PAOM is not being detected by the plug sample NMR system and that the fluid-filled porosity experienced some volumetric loss due to pulling the rock out of subsurface conditions. To test this hypothesis, we added the PAOM from DRA to the NMR porosity and compared that sum to the PhiT_DRA (Figure 7). This makes the two values closer, but the PhiT_DRA is still about 16% higher than PAOM-corrected NMR data. The most likely reason for the remaining difference is that the lab NMR system is not detecting all of the oil-filled pores and none of the gas-filled pores.

Three key findings from this study are:

1) multi-resolution SEM analysis can be used to quantify organic and non-organic porosity,

2) crushed rock total porosity may include a substantial clay-bound water volume that correlates to XRF clay volume,

3) dry helium porosity and SEM porosity plus computed clay-bound water porosity compare favorably,

4) fresh-state NMR total porosity plus SEM organic porosity best matched the clay-bound water corrected SEM porosity.

Summary and Conclusions

1. We investigate and define ‘corrections’ for multiple porosity techniques to arrive at the fully comprehensive answer that reasonably well agrees for all analytics applied; SEM-based image porosity to crushed rock porosity, and NMR based porosity to SEM-image and crushed rock porosity.

2. Fresh-state core sample NMR does not quantify the PAOM analytically. The use of SEM and NMR techniques together begins to unravel the quantification of all represented pore types at various scales to help understand the dominant contributing storage and flow properties of the formation in this study.

3. The combination of crushed rock, NMR, and SEM based porosity quantification allows us to petrophysically define the volume of organic-associated pore space and the intra-granular plus inter-granular pore space.

Selected References

Capsan, J., and J. Sanchez-Ramirez, 2016, Using Core Data, Digital Rocks, and Source Rock Kinetics to Reduce Hydrocarbon Storage Uncertainty in Unconventional Reservoirs: Application to South Texas Organic Rich Mudstones: Unconventional Resources Technology Conference, 1-3 August, San Antonio, Texas, URTEC 2461642, 20 p.

Chitale, V.D., 2010, Simplified and More Accurate Clay Typing Enhances the Value Added by Petrophysical Evaluation of Shale and Tight Gas Sand Plays: AAPG Convention, Denver, Colorado, June 7-10, 2009, Search and Discovery Article #40487 (2010). Website accessed August 2017.

Guidry, K., D. Luffel, and J. Curtis, 1995, Development of Laboratory and Petrophysical Techniques for Evaluating Shale Reservoirs: Gas research Institute, Chicago, Report GRI – 95/0496, 286 p.

Loucks, R.G., R.M. Reed, S.C. Ruppel, and U. Hammes, 2012, Spectrum of Pore Types and Networks in Mudrocks and a Descriptive Classification for Matrix-Related Mudrock Pores: American Association of Petroleum Geologists Bulletin, v. 96/6, p.1071-1098.

Luffel, D.L., F.K. Guidry, and J.B. Curtis, 1996, Development of Laboratory and Petrophysical Techniques for Evaluating Shale Reservoirs: Gas Research Institute Final Report GRI-95/0496 (October 1986–September 1993), p. 301.

Passey, Q.R., K.M. Bohacs, W.L. Esch, R. Klimentidis, and S. Sinha, 2010, From Oil-Prone Source Rock to Gas-Producing Shale Reservoir - Geologic and Petrophysical Characterization of Unconventional Shale-Gas Reservoirs: Chinese Petroleum Society/Society of Petroleum Engineers International Oil & Gas Conference and Exhibition, Beijing, China, June 8–10, 2010, SPE 131350, 29 p.

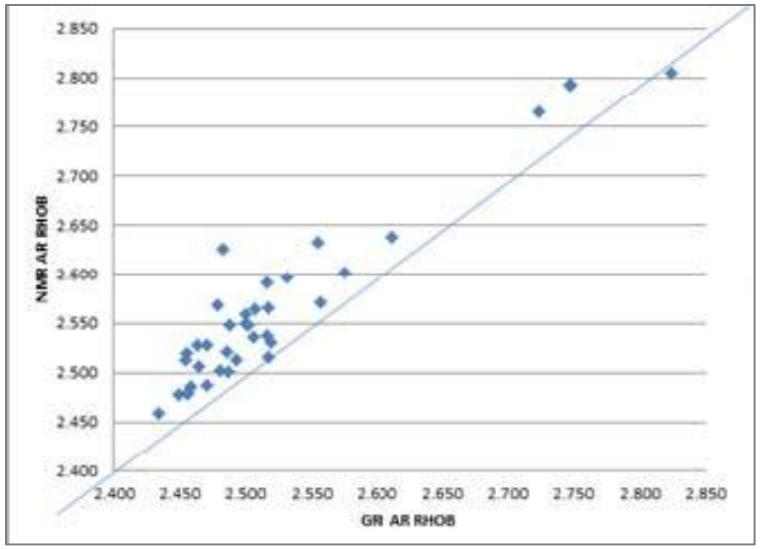

Figure 1. Analytical comparison of reported crushed rock bulk densities for analogous samples versus conventional plug samples bulk densities. Caliper-based measurements are consistently higher than Archimedes method bulk densities. At the time of the study, equipment and processing was limited to T2 relaxation therefore T1 polarization is not discussed or presented here.

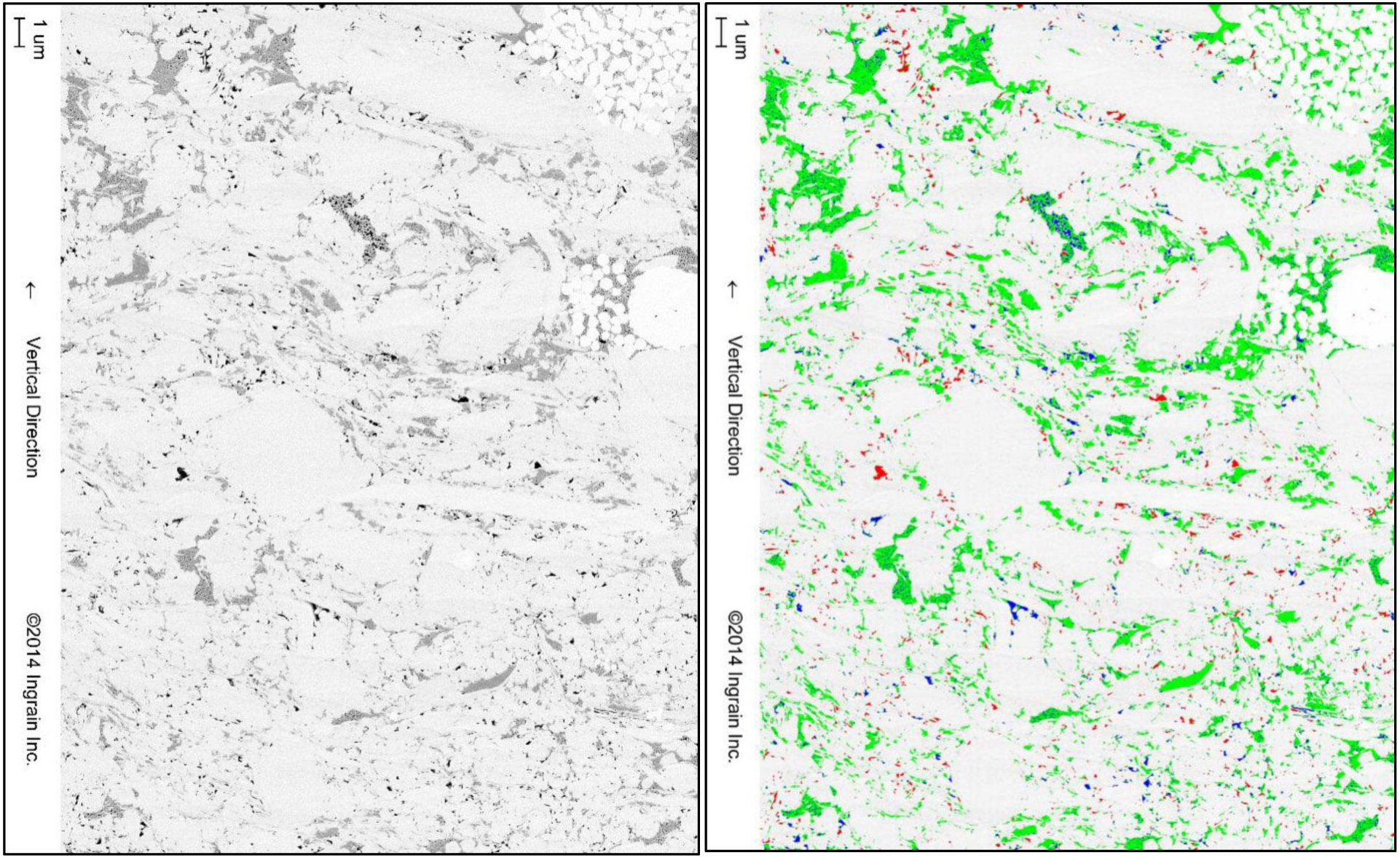

Figure 2A (left): One of ten secondary electron images per sample. Figure 2B (right): Same image is segmented with color shading for OM (green), PAOM (blue), and mineral-associated porosity (red).

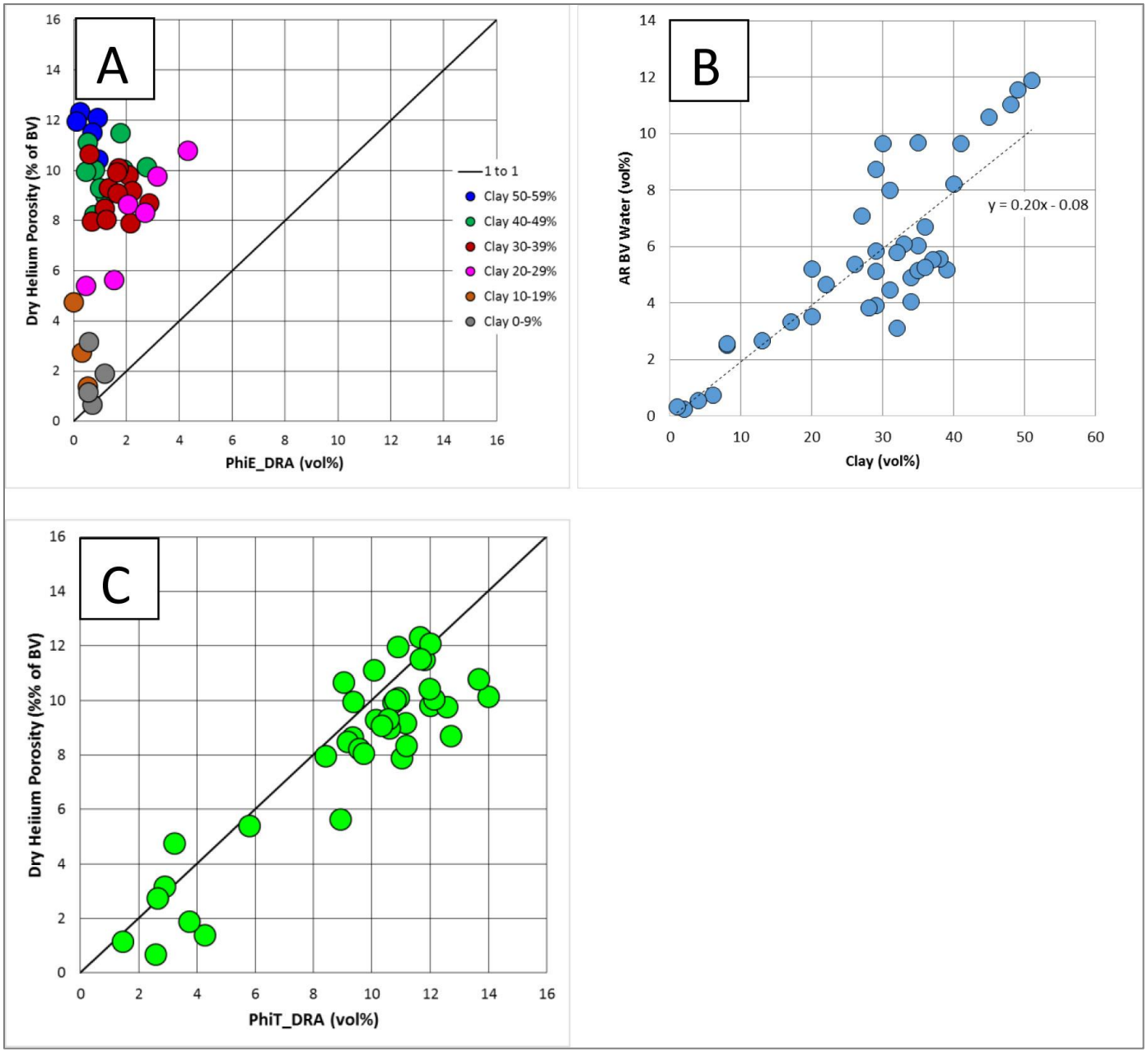

Figure 3A: Effective porosity measured from SEM images compared to Dry Helium Porosity. The samples were grouped by clay content and color coded accordingly. Figure 3B: Bulk volume water from Dean-Stark analysis on as-received samples compared to total clay volume from XRF. Figure 3C: Total SEM porosity compared to dry helium porosity. The total SEM porosity is computed from multi-resolution imaging and clay content.

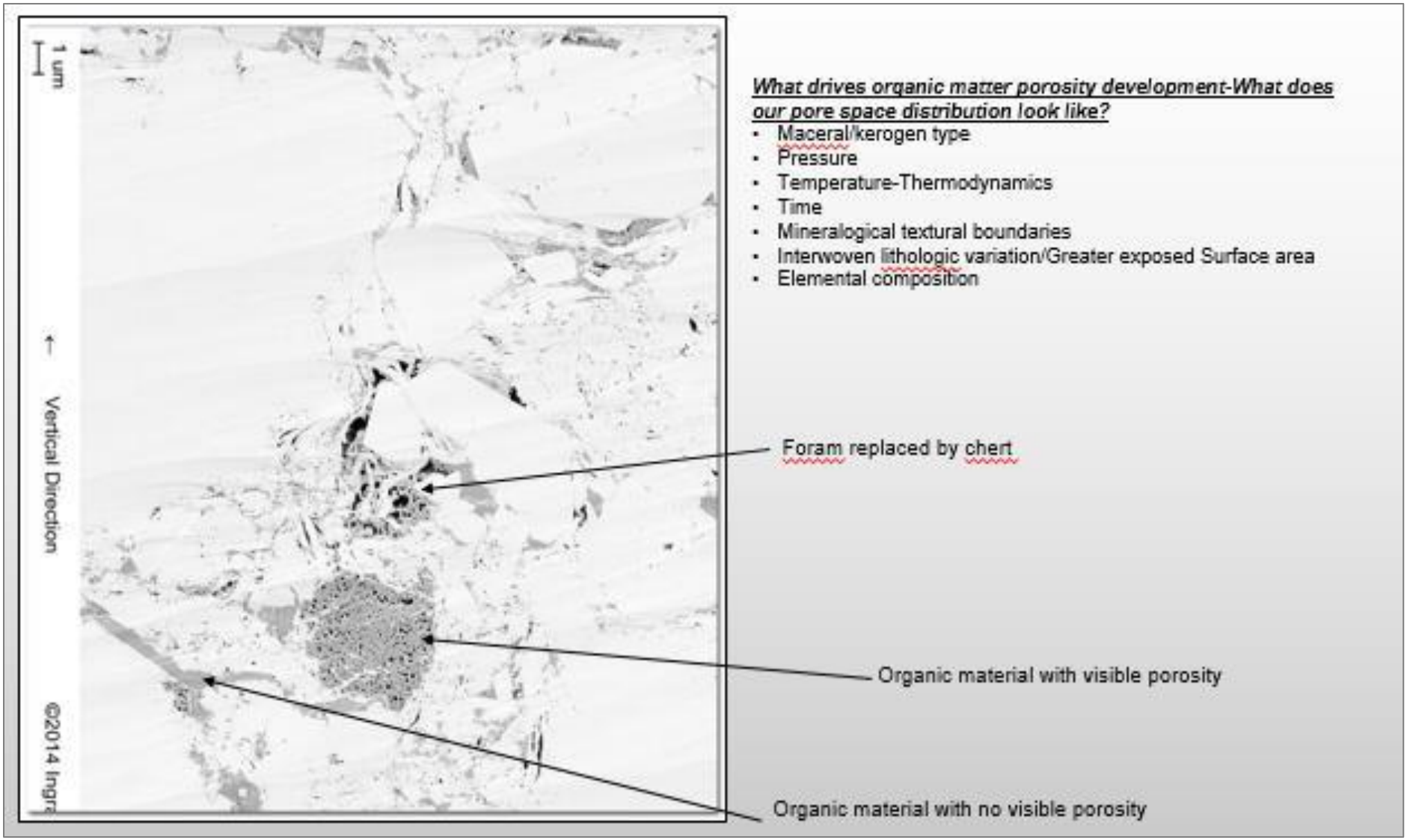

Figure 4. SEM image from this study depicting various mineral grain textural relationships and pore space for porosity quantification.

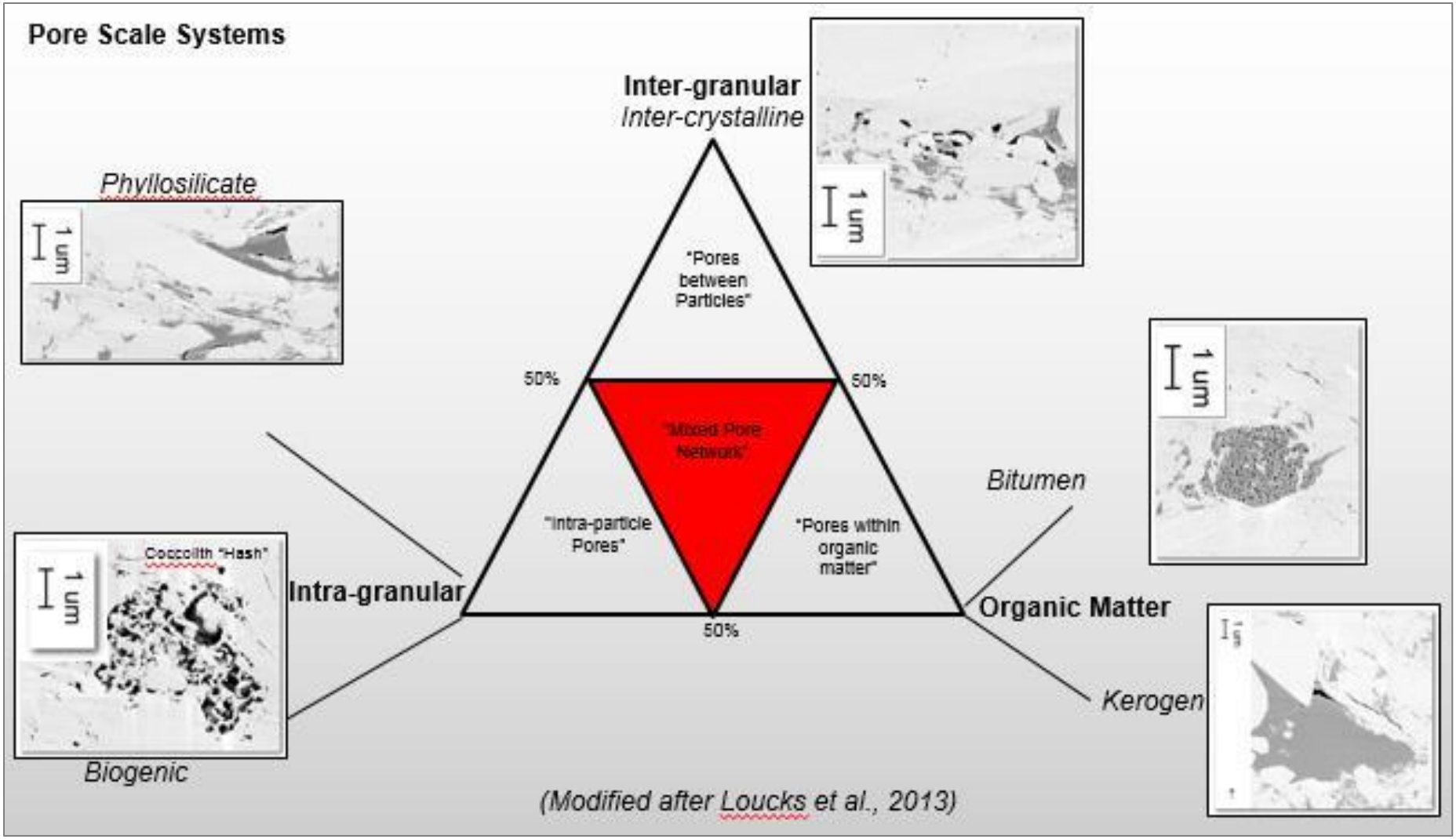

Figure 5. Modified after Loucks et al., 2015. SEM pore scale imagery from samples contained within this study shows a hybrid reservoir, predominantly phyllosilicate and intra- to inter-granular dominated.

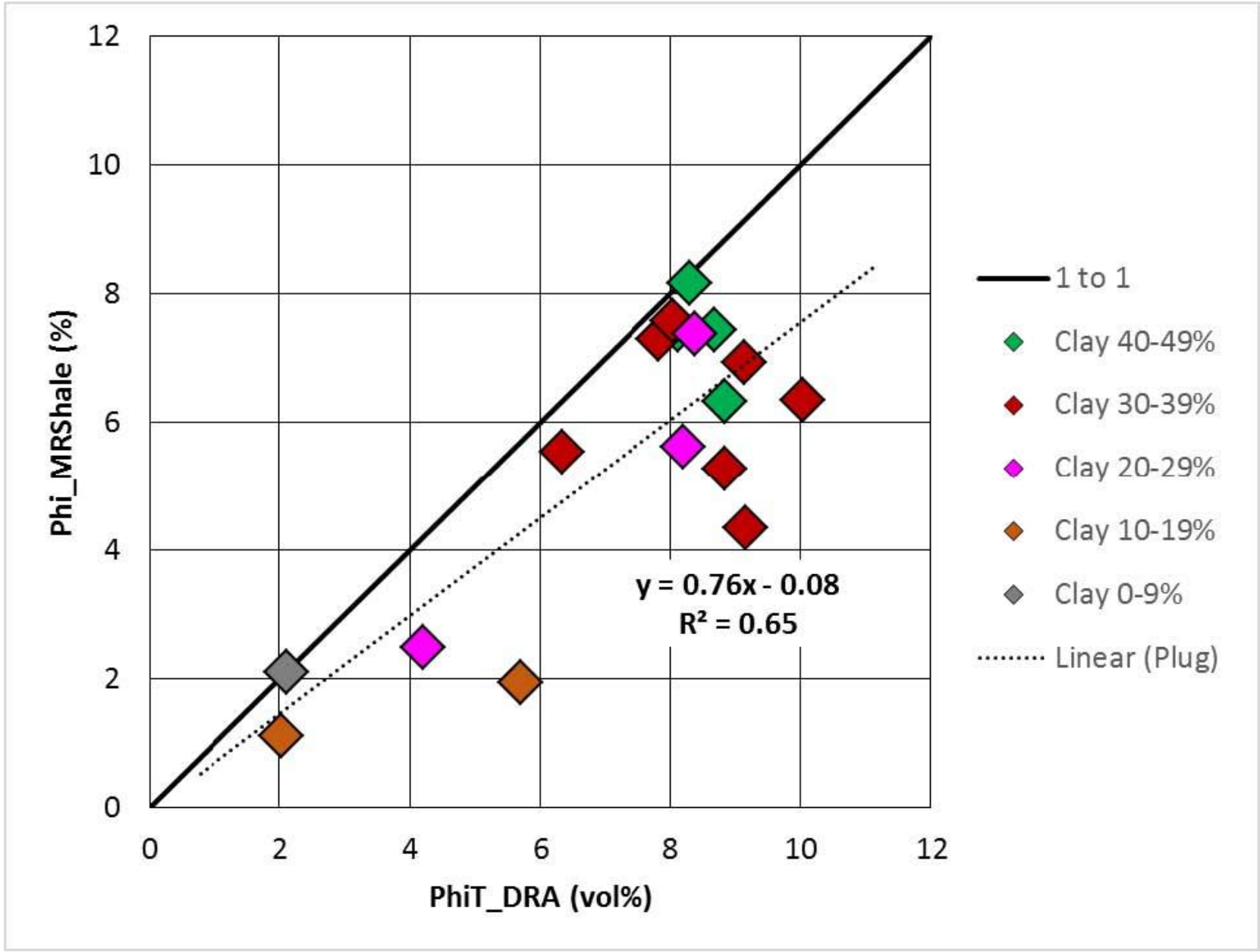

Figure 6. Comparison of the porosity from DRA and NMR porosity. The data points are color coded by clay content.

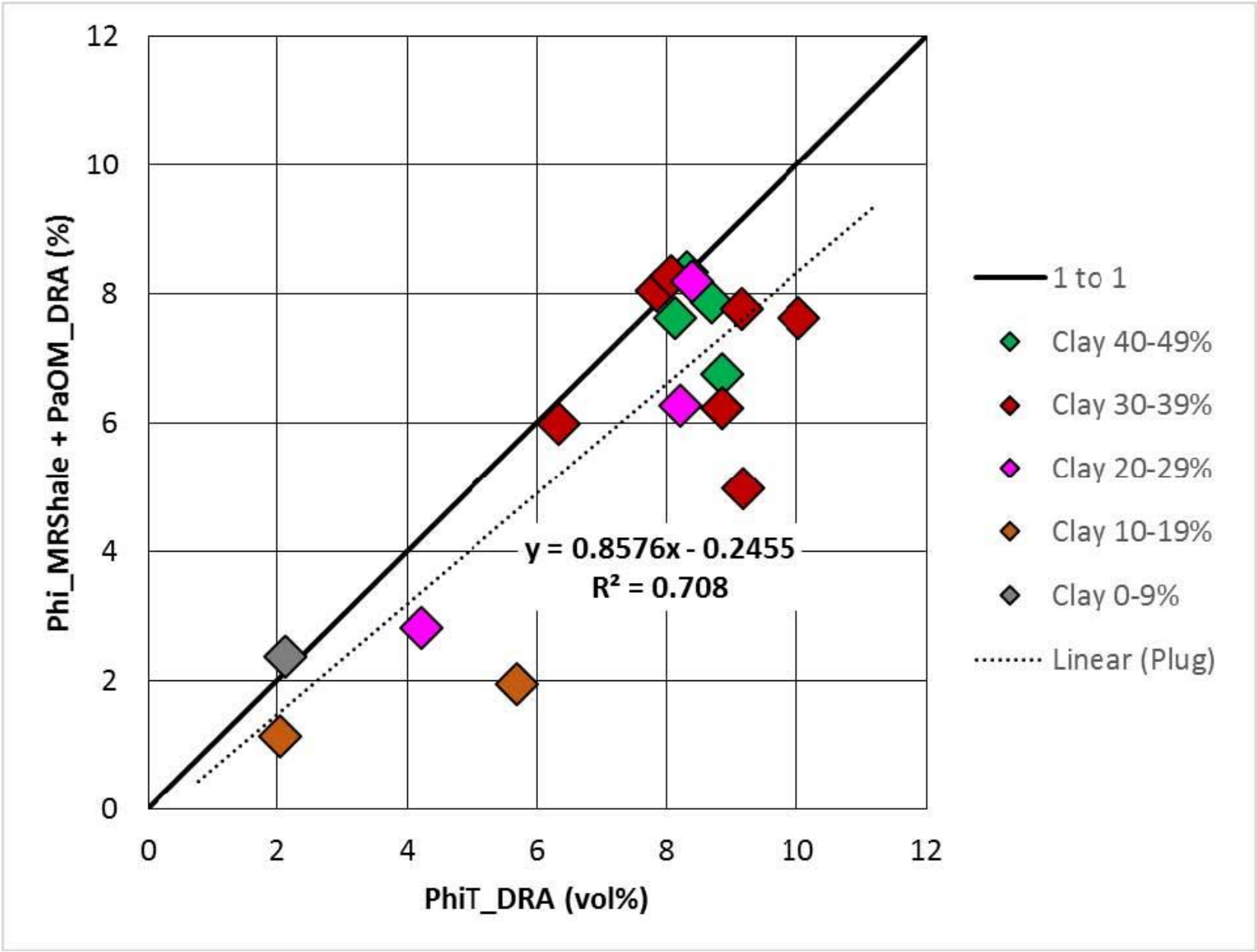

Figure 7. Porosity associated with organic material (PAOM) from DRA was added to the fresh-state NMR plug sample porosity. This figure shows the comparison of the porosity from DRA and the corrected NMR porosity.